

## Chapter Two

Clouds are not spheres, mountains are not cones, coastlines are not circles, and bark is not smooth, nor does lightning travel in a straight line.

-Mandelbrot, in his introduction to *The Fractal Geometry of Nature*

"Imagine the cow is a sphere...."

-Punchline to a joke about physicists.

*The most simple representation of a tree is the child-like image of a circular, photosynthetic surface supported by a perpendicular column. In general, the relationships of the above-ground organs of a tree can be described using the relationships  $M_s \propto M_T^\alpha$ ,  $M_L \propto M_s^\alpha$ ,  $D_s \propto M_s^\alpha$ , and  $H_s \propto D_s^\alpha$ . After basic mathematical relationships were determined, a game-like system was established in which each tree or propagule was treated as an object in a simulated world-space, where its ability to grow and survive was determined by the ability to harvest light.*

### **Code Considerations**

When conceptualizing how to model real-world events on a computer, an obvious difference between computers and reality is how events are handled. In the world we exist in, the universe can be seen as being massively parallel, with multiple things apparently happening at the same time. While there are various ways one can give the appearance that computers can do multiple things at once, in the absence of multiple processors, computers deal with things in a serial fashion, meaning that multithreading and other techniques for parallelization are just programmatic illusions (Neuburg, 1999, Tanenbaum, 1992). Such threads of execution occur when a program is forked into

more than one task. On a single processor, this multithreading occurs when the processor switches between different threads, incrementing each by a small amount. The amount of time spent incrementing each thread varies from language to language. For example, the Python programming language will, by default, execute 100 bytecode instructions before switching to the next thread (Martelli, 2005).

A fast enough computer can cycle through threads with such rapidity, executing each thread for a short period of time before stopping it and moving to the next, that the user has the illusion of parallelization (Neuburg, 1999). The effect is an illusion; effectively a zoetrope or praxinoscope.

This point may seem trivial and obvious, but it affects how one considers constructing the logic of a computer-based simulation, and has interesting philosophical implications. For example, we perceive the universe as being massively parallel with each and every subatomic particle behaving in ways independent from other subatomic particles (ignoring entanglement) (Figure 2.1). If, however, there were a conscious Actor existing within a serialized simulation, the Actor's perception of his universe would be that the universe was behaving in a massively parallel fashion. The simulation would cycle through each and every object in the simulated universe, making individual step-wise changes to each object's state. The Actor's perception, then, would last only as long as it was his 'turn'. The gaps of time between their perception would never exist from their relative perspective. The time between his 'turns' would be below his Planck time, a sort of persistence of consciousness.

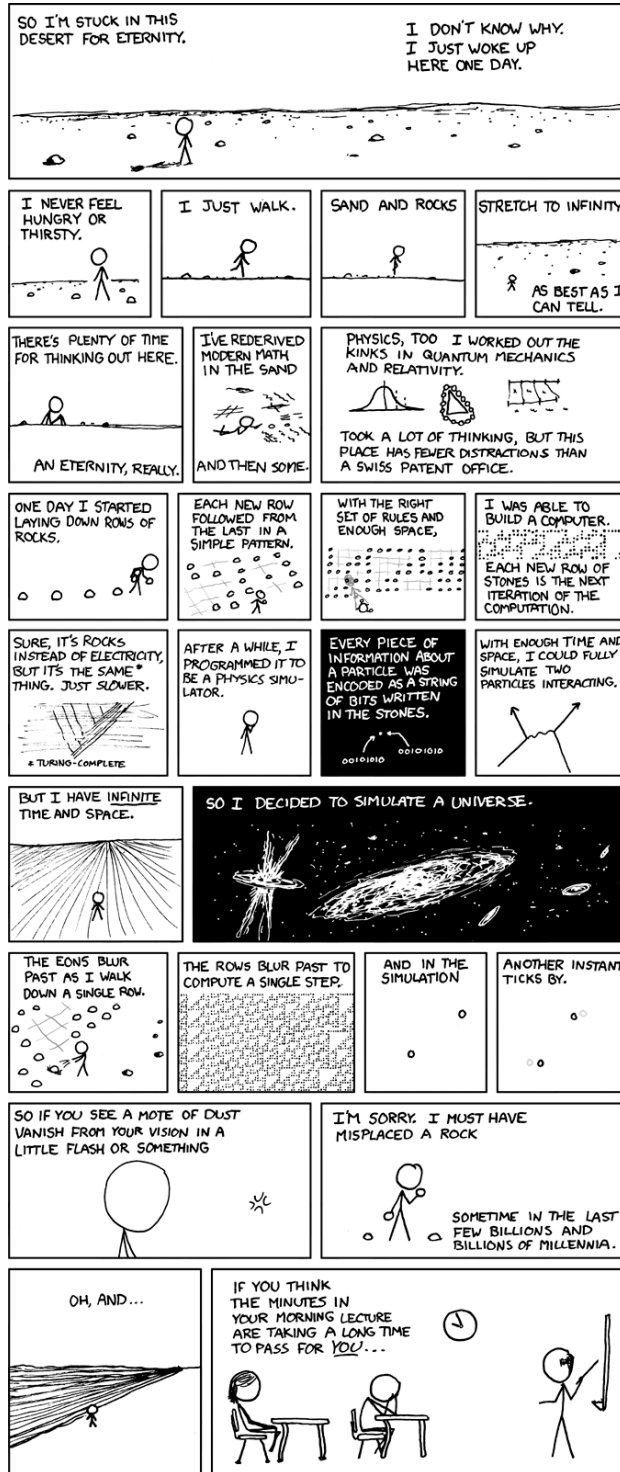


Figure 2.1 “A Bunch of Rocks”. Copyright Randal Monroe, XKCD. Used with permission.

In practice, implementing threads on a single processor, or implementing genuine parallel processing using multiple processors is a non-trivial situation. The third edition of “Programming Perl” makes the following analogy :

*Imagine taking a recipe from a cookbook and converting it into something that several dozen chefs can work on all at the same time. You can take two approaches.*

*One approach is to give each chef a private kitchen, complete with its own supply of raw materials and utensils. For recipes that can be divided into parts easily, and for foods that can be transported from kitchen to kitchen easily, this approach works well because it keeps the chefs out of each other’s kitchens.*

*Alternately, you can just put all the chefs into one kitchen, and let them work things out, like who gets to use the mixer when. This can get messy, especially when the meat cleavers start to fly (Wall, 2000).*

The former, individual kitchen model, is meant to represent the use of multiple processors, whereas the latter tries to model the multithreaded method using a single processor. While the number of personal computers that have multiple processors is increasing, the vast majority of older computers use a single processor. For this reason, the multithread model is the most common for now.

Some of the previous attempts at creating software to simulate individual and community interactions made use of SWARM, a multithreaded platform allowing individuals to create individual, interacting agents using code written in objective C (Enquist and Niklas, 2001a, 2001b; Pringle, 2001). Relatively simple in its implementation, the application referred to as PLANT was not parameterized using real world species data.

Rather than build upon this previous work, it was decided that all work should start from scratch, including envisioning how the program would deal with each object in the simulated world. To keep development relatively simple and somewhat easy to troubleshoot, it was decided to ignore parallel processing and multithreaded models. Instead, the program would run as a single thread, where each object in the world would be dealt with in a serial fashion.

Conceptualizing a simulation as running in a series of individual turns is quite easy to do, thanks in large part to the ubiquity of turn-based games in our culture. Envisioning a tree/forest-growth simulation in terms of a turn-based game allows one to sketch out a logical flow of events.

### ***The Game of Life***

Breaking down how an individual plant grows, one sees discrete steps:

- 1) Germination
- 2) Photosynthesis
- 3) Allocation of carbon to organs
  - 3a) Vegetative growth
  - 3i) Reproduction
  - 3ii) Seed dispersal

Simulating how an individual plant grows in its lonely platonic world is useful and informative, but one needs interactions between individuals if one wants to examine the results of competition for light and space on growth. When it comes to thinking about how plants in a simple world interact, the options are pretty limited: they kill one another.

Obviously a photosynthetic plant will die when it is deprived of light due to excessive shading. Plants in a simulation must also obey physical laws, e.g., they

cannot occupy the same space, and they cannot exceed their Euler-Greenhill maximum height.

Incorporating mortality into the simple flow chart yields:

- 1) Germination
  - 1a) Death due to failure to germinate
- 2) Photosynthesis
  - 2a) Death due to lack of light
- 3) Allocation of carbon to organs
  - 3a) Vegetative growth
    - 3i) Death due to Euler-Greenhill buckling.
    - 3ii) Reproduction
    - 3iii) Seed dispersal
  - 4) Other causes of death
    - 4a) Death due to the stem extending off the simulated world space.
    - 4b) Death due to being crushed
    - 4c) Death due to occupying the same space as another object.
    - 4d) Death due to senescence.
    - 4e) Stochastic death.

Creating realistic mortality algorithms is not a trivial process. A review of mortality algorithms by Hawkes showed just how complicated models can become (Hawkes, 2000). The source of this complication may arise from the fact that it is sometimes difficult to measure exactly why individuals die in natural, uncontrolled habitats. One can measure the number of trees that die within a hectare over a 10 year period, but what sort of bias does the data contain? Is the researcher only measuring the death of

trees that have a DBH (i.e. they are at least as tall as one's breast)? Do they somehow measure seedling mortality?

Even if an enterprising team of graduate students were able to record every tree death in a hectare, their ability of saying exactly why any given tree died would be difficult. If a tree is sickly, growing slowly in the shade, and dies due to a fungal infection, what is the cause of death? Lack of light or the fungus, or something else entirely?

In short, there are many, many ways to die in this world, and only a few ways to succeed.

To use the game analogy, one can imagine a software simulating growing trees as a modified Monopoly game. At the start of each player's (tree's) turn, they 'pass go' and collect a certain amount of money (carbon), based on the surface area of all the houses and hotels they have on the board. The player converts houses to hotels (allocates carbon to organs of the tree) and maybe places new houses on the board (reproduces). After each player has finished his turn, each player then picks up a gun from the Chance pile and plays Russian roulette to see who dies (due to stochastic death). The survivors then begin the next round.

With a simple game analogy in mind, the underlying relationships behind Vida were assembled.

### ***Modeling Very Simple Trees: Allometric Ideals and Spherical Cows***

With the eye of an artist and a desire for symmetry, Leonardo da Vinci formulated a means whereby he could generate realistic looking trees and plants in his works. In so doing, his observations are the first recorded instance of an individual using mathematical relationships to describe the form of a tree:

*All the branches of a tree at every stage of its height when put together are equal in thickness to the trunk [below them]....*

*Every year when the boughs of a plant [or tree] have made an end of maturing their growth, they will have made, when put together, a thickness equal to that of the main stem; and at every stage of its ramification you will find the thickness of the said main stem; as: i k, g h, e f, c d, a b, will always be equal to each other; unless the tree is pollard—if so the rule does not hold good.*

(Figure 2.2) (Richter, 1939)

This concept would be revisited and formalized in 1964 by Shinozaki et al., where they called Leonardo's rule-of-thumb the "pipe model" (Shinozaki et al., 1964a, 1964b). In the years that followed, thanks in large part to the work done by Mandelbrot (1982), the pipe model and the concept of iterative branching led to increasingly more realistic-looking computer generated images of trees and other plants (Weber, 1995; Lintemann, 1998; Deussen, 1998).

When one steps back from attempting to achieve realistic images of trees, an abstract "spherical cow" tree is exactly what a child might draw: a circular, photosynthetic surface supported by an elongated, perpendicular structural member. While a child's drawing might lack realism, it does capture the essence of a tree in its most basic, Platonic tree-ness. Attempting to split the difference between photorealistic images of trees and overly simple Platonic trees is problematic because robust information about the geometry of a tree canopy geometry is typically lacking in the datasets that also record information related to total tree mass, canopy mass, tree height, and other physical properties.

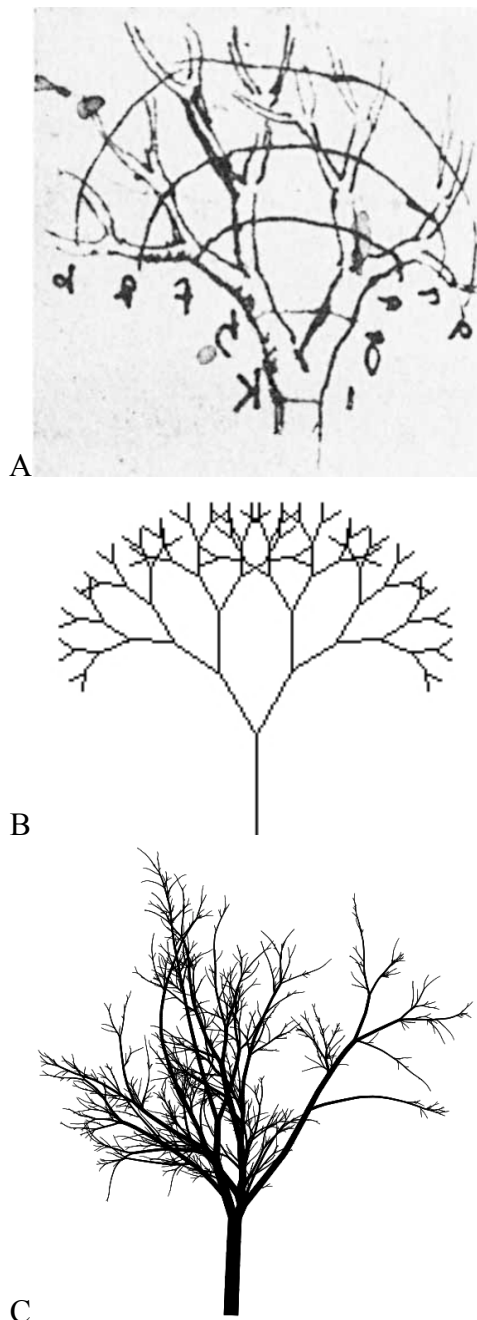


Figure 2.2: A.) Sketch from Leonardo's sketchbook. Labels (a-b, c-d, e-f, g-h, i-k) are in Leonardo's idiosyncratic backward handwriting. B.) A simple fractal tree. C.) A realistic looking, computer generated tree making use of fractal branching and reductions in stem diameters following the pipe model.

For the sake of simplification, if one assumes a tree's canopy acts as a uniformly thick surface, of which only one side is photosynthetically active, one can use easily obtained physical data and calculate the surface area according to the formula

$$A_L = \frac{M_L / \rho_L}{H_L} \quad (\text{Equation 2.1})$$

where  $A_L$  is the surface area ,  $M_L$  is the mass of the canopy,  $\rho_L$  is the density of the photosynthetic surface, and  $H_L$  is the thickness of the photosynthetic surface. If this area constitutes a flat surface parallel to the surface of the earth, the tree resembles a roofing nail. The canopy spread ( $R_L$ ) is arrived at using the equation:

$$R_L = \sqrt{\frac{A_L}{\pi}} \quad (\text{Equation 2.2})$$

While a wonderfully simplified tree, modeling the photosynthetic surface as a flat disc results in a canopy diameter that is relatively large. If one treats this same area as a hemisphere versus a flat disc, the radius is described as

$$R_{L_{\text{Hemisphere}}} = \sqrt{\frac{A_L}{2\pi}} \quad (\text{Equation 2.3})$$

If one assumes that light energy ( $E$ ) for photosynthesis comes from directly above each model tree, the area available to a 'roofing nail' type model is far greater than that available to the area available to a 'bumbershoot' type model, where the area available for photosynthesis is the projected area of the hemisphere.

$$A_{L_{\text{Projected}}} = \pi(R_{L_{\text{Hemisphere}}})^2 \quad (\text{Equation 2.4})$$

or

$$A_{L_{\text{Projected}}} = \frac{M_L}{2\rho_L H_L} \quad (\text{Equation 2.5})$$

Put another way, the area available for photosynthesis of a bumbershoot is half that

of a roofing nail.

One could more accurately model the geometry of a tree using prolate or oblate spheroids (or as cones in the case of some conifers) and achieve more realistic canopy spreads, but a hemispherical model is relatively easy to work with mathematically if one is striving for the most simple model.

The mass of the canopy and the structures that elevate it are governed by the following relationships:

$$M_S \propto M_T^\alpha$$

$$M_L \propto M_S^\alpha$$

$$D_S \propto M_S^\alpha$$

$$H_S \propto D_S^\alpha$$

In the early part of the 20<sup>th</sup> century, Huxley observed that such relationships are often linear when plotted on log-log paper, and took the form of  $Y = \beta X^\alpha$  (where beta is a species-specific constant and alpha is the slope of the line) and is similar despite differences in species (Huxley, 1932). While the observation is interesting, an underlying reason as to why these relationships exist has remained elusive (Niklas, 1994, 2004; also see Chapter 1). Huxley's generalization has allowed for the creation of practical databases, however. Foresters and ecologists have made use of various formulae that allow them to estimate a given tree's total above-ground mass, mass of the trunk and stems, mass of the canopy, and height, based on a tree's DBH (Jenkins, 2004; Zianis 2005; Navar, 2009).

$$M_S = \beta_1 D_S^{\alpha_1} \quad (\text{Equation 2.6})$$

$$M_L = \beta_2 D_S^{\alpha_2} \quad (\text{Equation 2.7})$$

$$H_S = \beta_3 D_S^{\alpha_3} \quad (\text{Equation 2.8})$$

The vast majority of studies examining the allometry of trees fall into two

categories: those that attempt to show underlying allometric trends among all species, and those that are interested in the practical application of allometry to help predict standing biomass. In the former case, species encompassing numerous genera are often grouped together, while in the latter case, specific formulae are constructed for each species and rely on the DBH as the dependant variable. Relationships based on the DBH are useful in a practical sense in that a tree trunk's diameter is the easiest physical characteristic that can be measured in the field in a nondestructive fashion. However, reliance upon DBH creates a situation that does not reflect a logical flow of carbon in an organism.

The following formulae are better suited to show the flow of carbon within a tree:

$$M_S = \beta_4 M_T^{\alpha_4} \quad (\text{Equation 2.9})$$

$$M_L = \beta_5 M_S^{\alpha_5} \quad (\text{Equation 2.10})$$

$$D_S = \beta_6 M_S^{\alpha_6} \quad (\text{Equation 2.11})$$

$$H_S = \beta_7 D_S^{\alpha_7} \quad (\text{Equation 2.12})$$

While generally correct, Equation 2.12 is observably incorrect. A tree's diameter will continue to increase over the entire course of its life (thus the ability to use tree rings to determine a tree's age), but trees do not continue to grow in height indefinitely. Even the tallest species of trees have limits on their height imposed by their ability to transport water to the highest boughs. Careful observation has shown that the relationship between diameter and height is more accurately portrayed by

$$H_S = \beta_7 D_S^{\alpha_7} - \beta_8 \quad (\text{Equation 2.13a})$$

and

$$H_S = \beta_9 + \beta_{10} \ln D_S \quad (\text{Equation 2.13b})^5$$

---

<sup>5</sup> Interestingly, the right hand side of the equation for height is essentially the same as Ludwig Boltzmann's formula for entropy:  $S = k \ln W$ .

where Equation 2.13a models a growth early in a tree's life when the amount of secondary xylem is minimal within the entire tree, and Equation 2.13b models an increasing amount of secondary xylem and dead heartwood. Because very small values of  $D_S$  can result in negative values of  $H_S$  in equation 2.13b, the transition point from equation 2.13a to 2.13b occurs when equation 2.13b results in a value for  $H_S$  that is greater than or equal to the value for  $H_S$  arrived at by using equation 2.13a. (Figure 2.3)

Another slightly more complex relationship involves the relationship  $M_L \propto M_S$ . While the general equation  $Y = \beta X^\alpha$  is still valid, it appears there are at least two different relationships (as shown in Figure 2.4):

$$M_L = \beta_5 M_S^{\alpha_5} \quad (\text{Equation 2.14a})$$

$$M_L = \beta_{11} M_S^{\alpha_8} \quad (\text{Equation 2.14b})$$

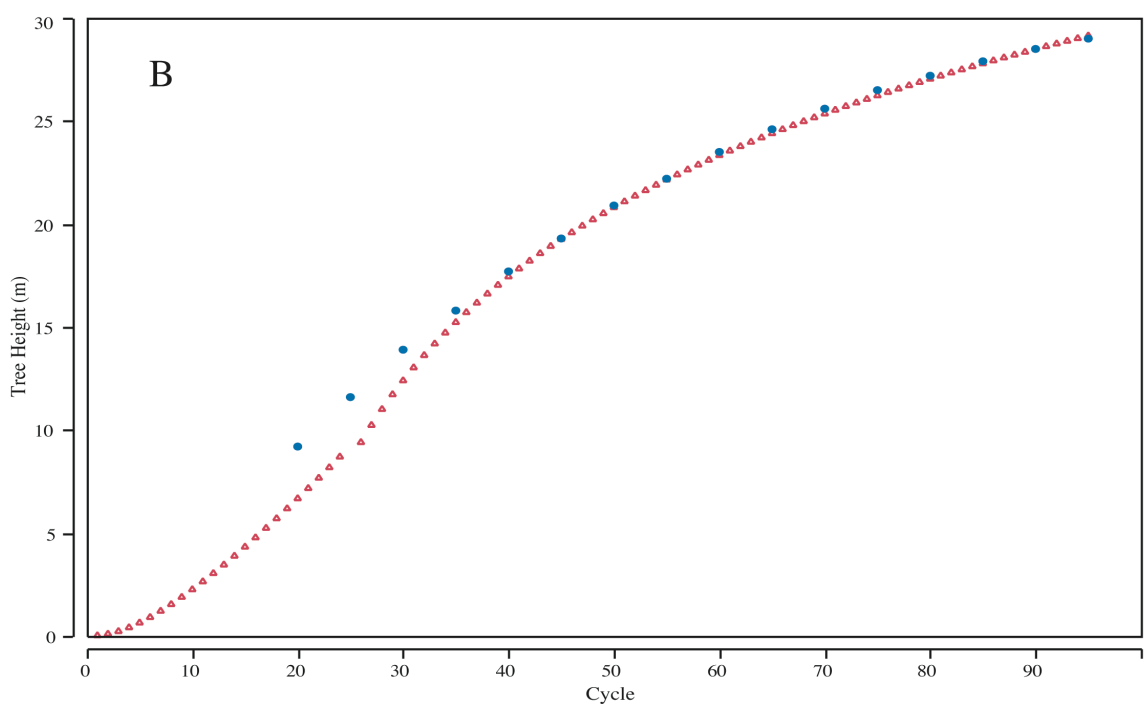
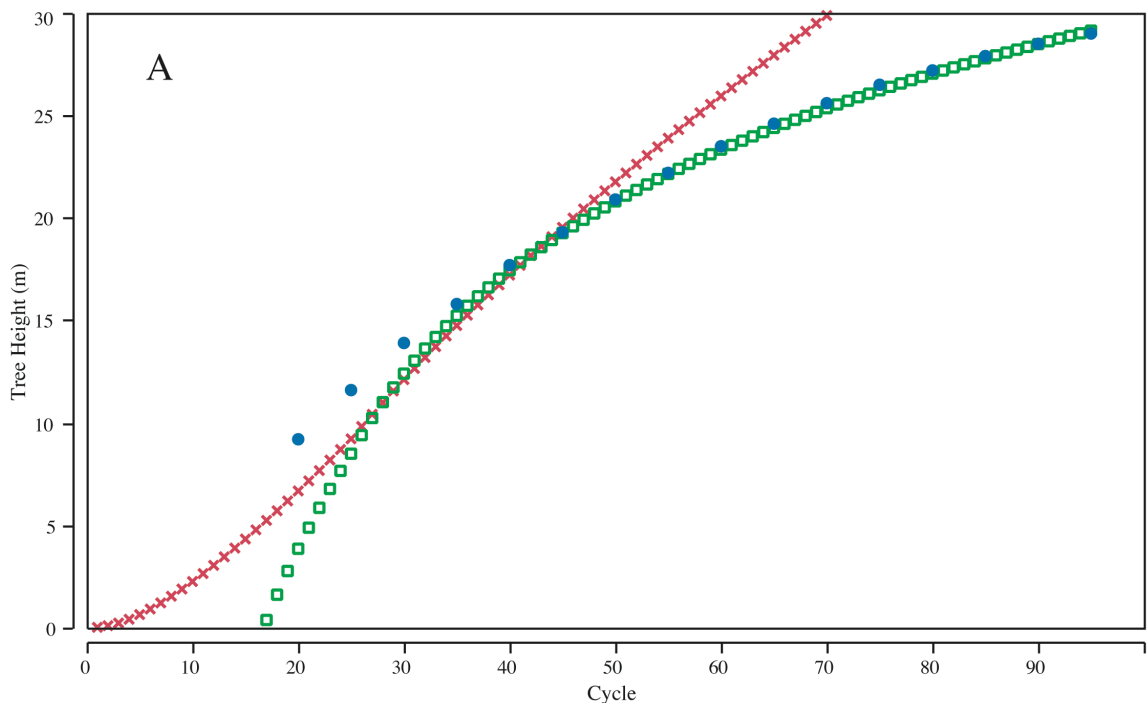
A similar trend was reported by Huxley (1932) for male *Uca pugnax* (fiddler crabs), in his seminal "Problems of Relative Growth." Huxley illustrated how the mass of the male's large chela in relation to the total body mass was closely approximated by the formula  $Y = \beta X^\alpha$ :

*The best worked-out example of this law so far concerns the large chela of male fiddler-crabs, Uca pugnax. This obeys the law of constant growth-ratio from crabs of only about 60 milligrams total weight to the largest found, weighing sixty times as much; the value for  $k^6$ , however, changes quite abruptly at about 1.1g total weight, a point which probably denotes the onset of sexual maturity, decreasing here to less than 80 per cent. of its value for the earlier growth-phase.* (Huxley, 1932)(Figure 2.5)

---

<sup>6</sup> Huxley's early work designated the variable  $k$  as being the exponent in the power law equation he became associated with. It wasn't until 1936 that Huxley advocated using the form  $Y=bX^\alpha$ . See Chapter 1.

Figure 2.3: A) Actual growth data from a managed stand of *A. alba* plotted in blue (Cantiana, 1974). Simulated growth using a simple Microsoft Excel based simulation using Equation 2.13a plotted in red. Simulated growth using a simple Microsoft Excel based simulation using Equation 2.13b in green. B) Actual growth from a managed stand of *A. alba*, plotted in red, compared to a combined Microsoft Excel based simulation where growth transitions from using Equation 2.13a to 2.13b once the value of 2.13b exceeds the value of 2.13a.



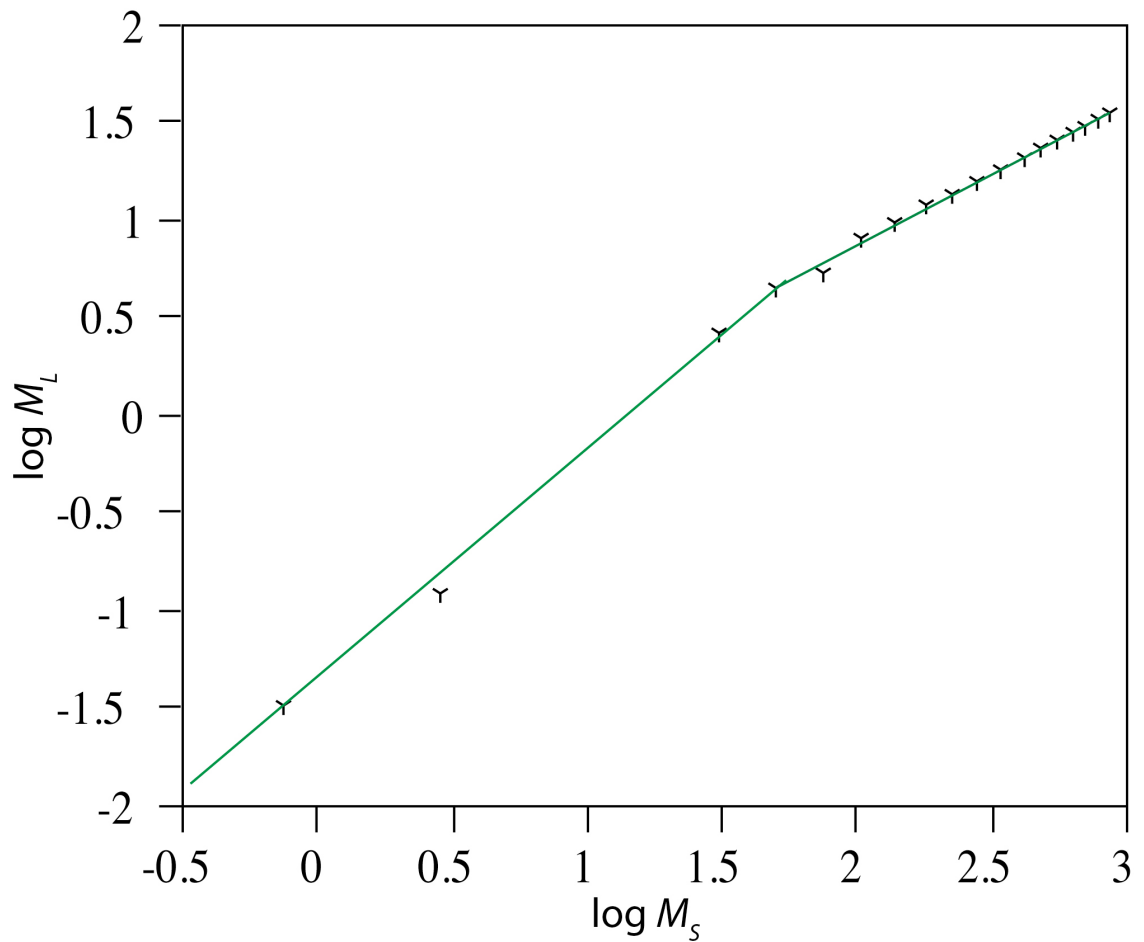


Figure 2.4: Data drawn from the Cannell data set showing the relationship between the mass of the canopy ( $M_L$ ) and the mass of the trunk and branches ( $M_s$ ) of a stand of *A. alba*, illustrating a change in the slope of the line.

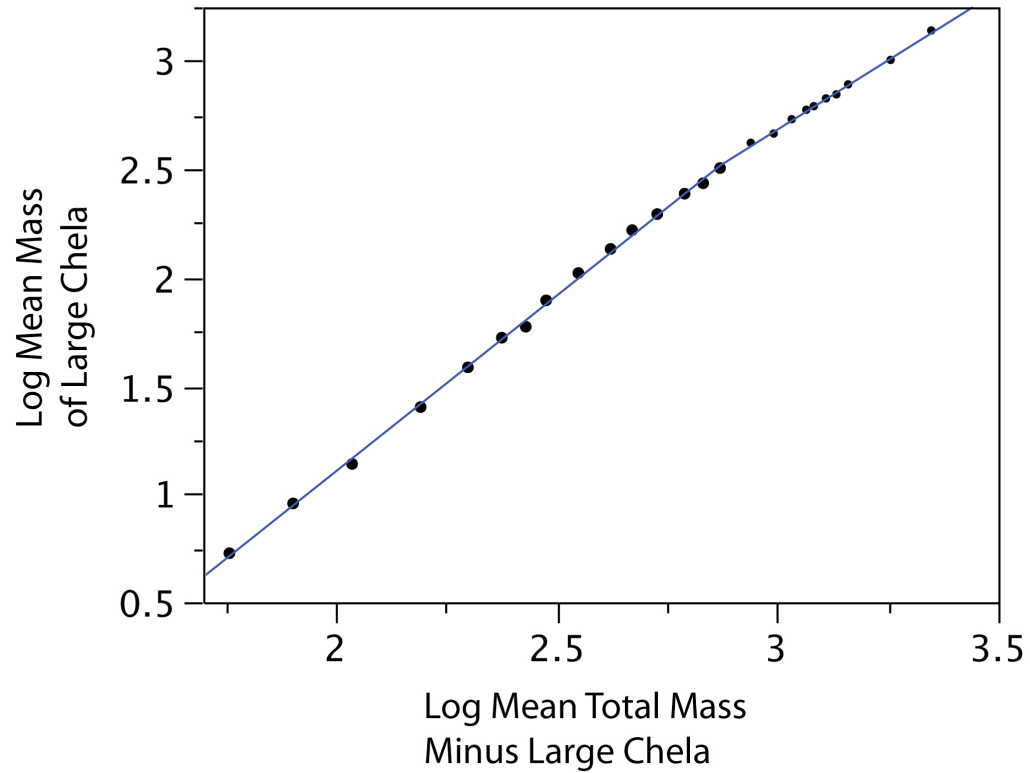


Figure 2.5: Log-log plot of data originally presented by Huxley, showing the relationship between the mass of the large chela and mass of the body of *U. pugnax*, illustrating a change in the slope of the line. (Huxley, 1932).

An individual tree's relationship between  $M_L$  and  $M_S$  is clearly not a single line but, like the *U. pugnax* chela vs. body mass relationship, it "changes quite abruptly." The exact cause for this shift within trees is not necessarily transparent when one examines large datasets, and it can be completely obscured if one combines data for populations (even of the same species) growing in differing geographic locations.

The perception that  $M_L \propto M_S^\alpha$  or  $H_S \propto D_S^\alpha$  are log-log linear emerges from studies in which multiple genera are grouped together. While useful to ascertain cross-species trends, differences between individual species become noise lost in the analysis. Take, for example, data on human growth provided by the United States' National Center for Health Statistics (Centers for Disease Control and Prevention, 2000). Due to sexual dimorphism, merging data for male and female growth patterns results in a poor model to approximate either male or female growth, but would allow one to conceptualize what a "human" growth model would be (Figure 2.6). Including other closely related species, such as *Pan trogloditis*, *P. troglodytes*, *P. paniscus*, *Gorilla gorilla* and *G. beringei*, one can generate a model for the living Hominidae, but such a model would obviously be poor at predicting the growth of a *Homo sapiens* male.

Thus, one can continue to add more and more data to an analysis, making it more and more inclusive. While informative as to general trends, such an amalgam of data can never accurately model any real species; instead, it shows an abstractly useful—but practically deceptive—average. In general, one can best see the transitions in  $M_L \propto M_S^\alpha$  or  $H_S \propto D_S^\alpha$  relationships when one examines a specific population growing in the same geographic location so that all individuals are experiencing the same environmental fluctuations.

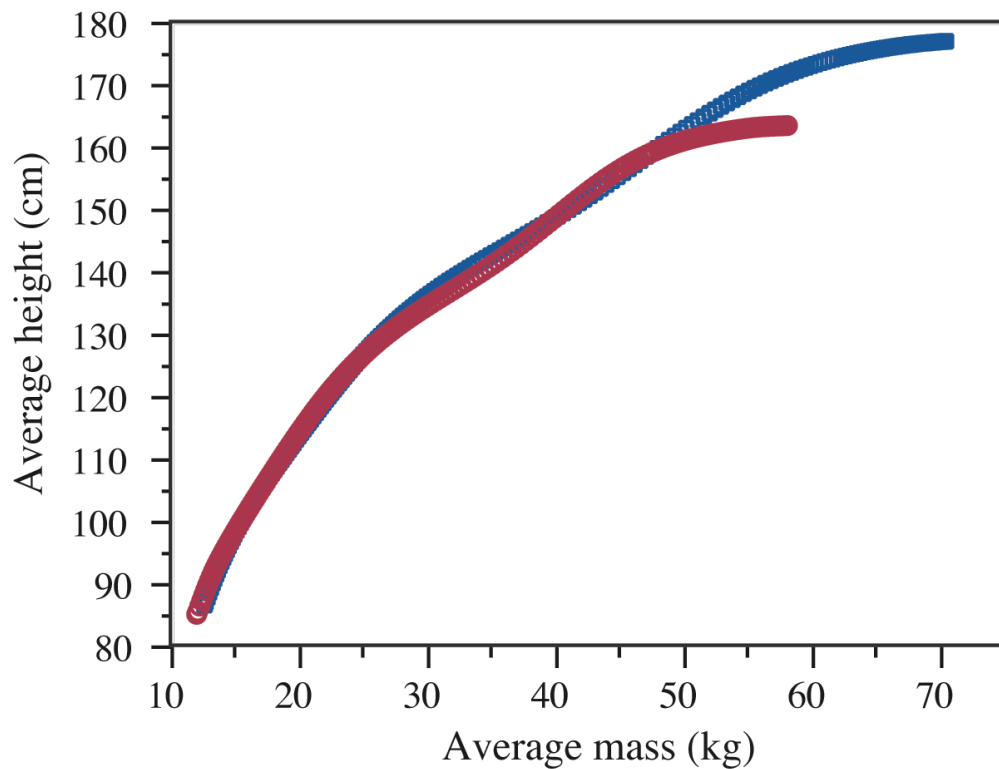


Figure 2.6: Comparison of the growth of male (blue) and female (red) *Homo sapiens* height compared to increase in mass. Combining the two datasets would result in an accurate model of human growth, but would lack information relevant to modeling sexual dimorphism within the species.

Taking into account the minor changes in formulae to make them mirror reality more accurately, the four basic equations showing carbon allocation in the above-ground portions of a tree are

$$M_S = \beta_4 M_T^{\alpha_4} \quad (\text{Equation 2.9})$$

$$M_L = \beta_5 M_S^{\alpha_5} \rightarrow M_L = \beta_{11} M_S^{\alpha_8} \quad (\text{Equation 2.14a and b})$$

$$D_S = \beta_6 M_S^{\alpha_6} \quad (\text{Equation 2.11})$$

$$H_S = \beta_7 D_S^{\alpha_7} - \beta_8 \rightarrow H_S = \beta_9 + \beta_{10} \ln D_S \quad (\text{Equation 2.13a and b})$$

A physical aspect of plants that has not been touched on concerns their reproductive structures. Different plant species have evolved vastly different details in how they reproduce. Clonal reproduction via plantlets, seed-filled cones, nuts, and fruits are only a few of the myriad ways in which plants have found effective ways to reproduce. With such a diverse set of reproductive structures, the word *propagule* encompasses all of these structures.

The propagules produced on the Platonic trees described here can be very simply represented as spheres. Their diameter ( $D_P$ ) is calculated using the species-specific values for propagule density ( $\rho_P$ ) and mass ( $M_P$ )

$$D_P = \left[ \frac{M_P}{(4/3)\pi\rho_P} \right]^{1/3} \quad (\text{Equation 2.15})$$

### ***Germination —***

Different plant species have evolved vastly different details in how they reproduce. Clonal reproduction via plantlets, seed-filled cones, nuts, and fruits are only a few of the myriad ways in which plants have found effective ways to reproduce. With such a diverse set of reproductive structures, the word *propagule*, as noted, will be used within this work to encompass all of these structures.

All plants simulated by Vida begin as propagules. Whether a propagule germinates depends on three factors: (1) a pseudo-random chance of death related to what fraction of seeds fail to germinate, (2) if seed mass is larger than a critical minimum value, and (3) whether a species is characterized as having delayed germination.

Factor (1) is optional in that the default setting is to ignore germination failure during the initial iteration. Factor (2) is also optional because simulations are initialized with propagules that have the correct mass for any given species. The only time factor affecting a run is when plants in the simulated world begin making and dispersing their own propagules. Factor (3) is explicitly defined for each species (most species have a germination delay set to 0, i.e., germination occurs in the first year).

Assuming a propagule can germinate, a series of simple calculations is used to determine exactly what fraction ( $\phi$ ) of its mass ( $M_D$ ) is converted to the newly germinated plant ( $M_T$ ), and how much of the seedling's mass is stem ( $M_S$ ) and canopy ( $M_L$ ), i.e.

$$M_T = \phi_1 M_P \quad (\text{Equation 2.16})$$

$$M_S = \phi_2 M_T \quad (\text{Equation 2.17})$$

$$M_L = M_T - M_S \quad (\text{Equation 2.18})$$

### ***Vegetative growth —***

The size of the canopy, and the extent to which it is shaded by neighboring plants, dictates the ability of the individual to harvest light and thus grow. Vida assumes that all light energy ( $E$ ) comes from directly above each plant and that light interception is time-averaged over a year, i.e., the unit of time in any iteration  $i$ .

Attenuation of  $E$  as it passes through a tree's canopy ( $E_T$ ) is an important component regulating whether or not understory plants can survive. At one extreme, if no light reaches the ground, no plants can survive until a gap appears in the forest due to the

death of a tree. The reality is that some light will filter through canopies, so an understory plant's ability to survive rests on its shade tolerance and just how much light passes through the canopy.

While there is information available about the shade tolerance of various species, it is often presented as a relativistic measurement (Nienemets and Valladares, 2006). What is known is that approximately 20% of full sunlight passes through a single tree's canopy and reaches the ground (personal communication with Dr. Thomas Owens, Cornell University). Therefore, is it reasonable to assume a 20% transmission rate for simulated tree canopies, and that, if a tree receives less than 20% of  $E$  in a simulation, it should die due to lack of light. Calculations on how shaded a given plant might be are complicated in that it can be partly or wholly shaded by one or more overtopping canopies.

The best solution to calculate the amount of light energy ( $E$ ) reaching a plant is to use a Monte Carlo method in which a fixed number of 'photons' are moved through the  $z$ -axis (Wilson, 1983; Prahl, 1989; Hasegawa, 1991). Every time a photon encounters a canopy, there is a fixed chance whether or not it will continue to move downward in the  $z$ -axis, or be 'absorbed'. For example, if a canopy allows 20% of the light to pass through it, than, on average, two out of every ten photons in the axis corresponding to the location of a canopy will continue downward. For the sake of simplifying calculations, we can assume that there is no light scattering in the atmosphere or in tissues, so photons only move from  $+z$  to  $-z$ .

To implement this concept, a given tree's canopy is first bounded by a box and all trees the same height or taller than the target tree are tested to see whether their canopies overlap partly or wholly. Next, a series of 'photons' are generated within the bounding box, having a  $z$  value greater than the highest tree canopy. Photons with  $x$ ,  $y$  coordinates falling outside the canopy area of the test tree are removed and the  $z$ -axis of

the remaining ones are set to the tallest tree. All trees have a value defining how much light passes through their canopy ( $E_T$ ) and, if a given photon intersects a given tree, it has a  $(E_T)^*100\%$  chance of continuing. The remaining photons are set to the next lowest canopy height and again tested. After all photons reach the target tree, one can determine how shaded the tree is by comparing the total number of photons reaching the tree with the starting number of photons. If, for example, 500 photons begin at  $z_{\max+1}$  and 250 photons reach the  $z$ -axis at which the tree's photosynthetic surface is located, the tree is 50% shaded.

The maximum possible photosynthetic area per plant is the projected surface area of the canopy ( $A_L$ ), and the annual growth ( $G_{T_i}$ ) equals the sum of the change in leaf mass per year ( $dM_L/dt$ ) and the change in stem mass per year ( $dM_S/dt$ ). The conversion of  $E$  into growth per iteration is described by

$$G_{T_i} = E A_L (\beta_{12} M_L^{\alpha_9}) \quad (\text{Equation 2.19})$$

where  $\beta_{12}$  and  $\alpha_9$  denote a species-specific normalization (allometric) constant and scaling exponent, respectively,  $A_L$  is the projected canopy area, and  $E$  is a fraction of full sunlight reaching the photosynthetic surface (Figure 2.7).

Growth in biomass is subsequently partitioned into new stem and canopy mass using the formulas

$$M_{S_i} = M_{S_{i-1}} + \beta_4 G_{T_i}^{\alpha_4} \quad (\text{Equation 2.20})$$

$$M_{L_i} = \beta_5 M_{S_i}^{\alpha_5} \rightarrow M_{L_i} = \beta_{11} M_{S_i}^{\alpha_8} \quad (\text{Equation 2.14a and b})$$

where the subscript  $i - 1$  denotes mass in the previous iteration of growth (which for a propagule is specified when a simulation is initiated; see ***Germination***). Equations 2.19, 2.20 and 2.14(a and b) are reiterated for each growth cycle. It is important to note that using Equations 2.14(a and b) and 2.20 to calculate  $M_S$  and  $M_L$  typically stipulates

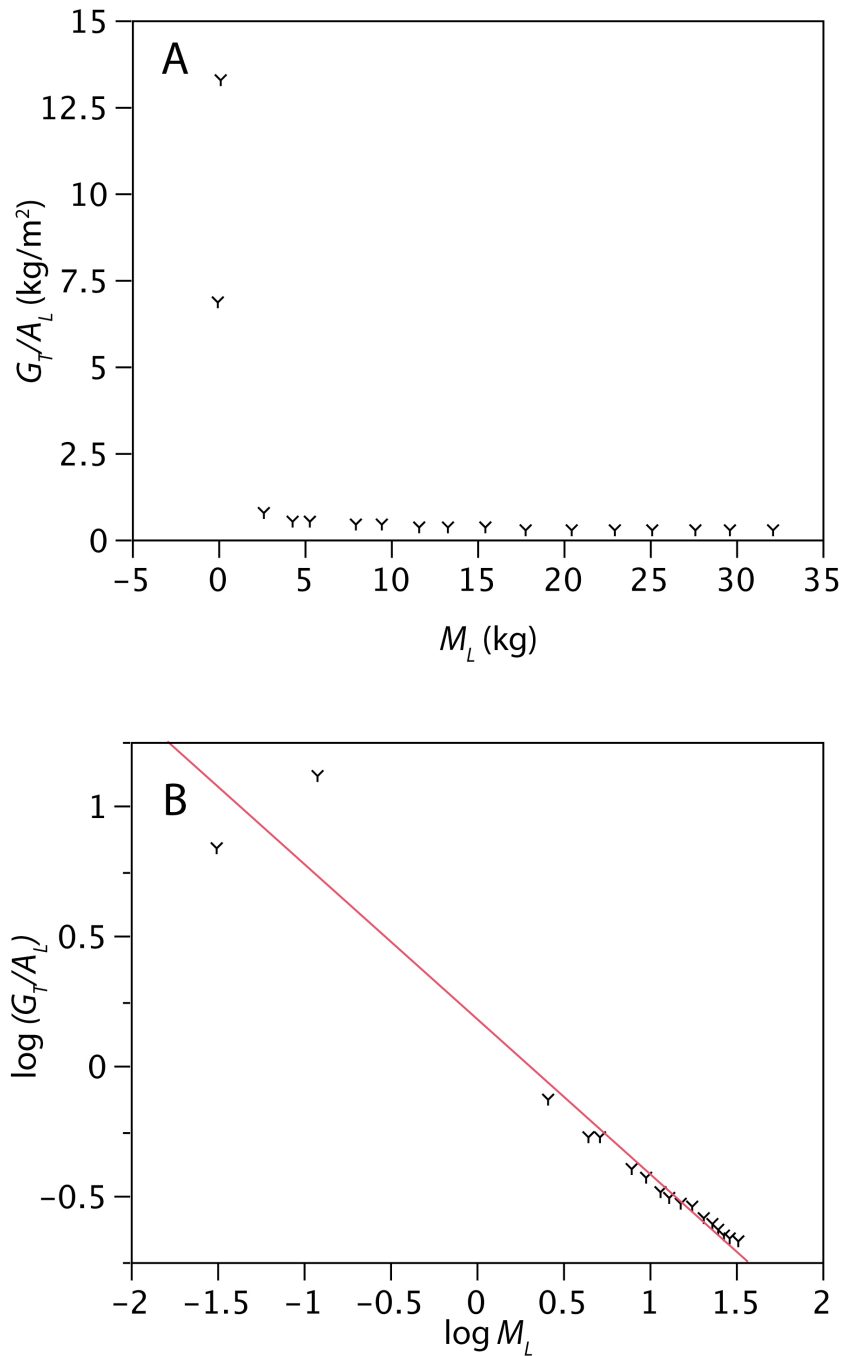


Figure 2.7: Total growth divided by projected surface area of the canopy ( $G_T/A_L$ ) versus the mass of the canopy ( $M_L$ ) of a managed forest of *Abies alba*. A: simple plot of  $G_T/A_L$  versus  $M_L$ . B: log-log plot of  $G_T/A_L$  versus  $M_L$ , where the fit line is described

by  $G_{T_i} = E A_L \left( \beta_{12} M_L^{\alpha_9} \right)$  where  $E$  is equal to 1.0.

that  $M_S + M_L \neq M_T$ . Rounding errors and incomplete field data are the source of this error.

For each iteration, Vida uses  $G_{T_i}$  to determine changes in  $M_S$ ,  $M_L$ ,  $D_S$  and  $H_S$ . As Equation 2.13 indicates, there is a shift in how  $H_S$  is calculated. This shift occurs in the iteration after the condition  $H_{S_b} > H_{S_a}$  has been reached. Computer runs and allometric analyses of data from real species indicate that this shift occurs when a species becomes reproductively mature.

When species become reproductively mature, a second shift in growth occurs for the mass allocated to the canopy, using Equation 2.14a for young plants and using Equation 2.14b for older plants once the software begins using 2.13b to calculate plant height.

### ***Propagule Production, Location and Dispersal***

A number of questions need to be addressed when simulating plant reproduction: what factors trigger the onset of sexual maturity? How much carbon is diverted toward reproductive efforts? What is the mass of a propagule and how many are produced? Where are the reproductive units located upon the mother plant? How are they dispersed? The answers to these questions differ from species, but insights that allow models to be made.

### ***Onset of Maturity***

As had previously been discussed, Huxley hypothesized that the abrupt change he observed in *U. pugnax* chela mass, relative to the mass of the rest of the body (Figure 2.5), had to do with the onset of sexual maturity (Huxley, 1932). The a similar change is observed in the  $M_L$  relative to  $M_S$  for individual species, as described by Equation 2.14 (Figure 2.4), and in the relationship between  $D_S$  and  $H_S$ , as described by Equation 2.13 (Figure 2.3). The point at which Equation 2.13b results in values for  $H_S$  that

exceed those from Equation 2.13a coincides with the transition described by Equation 2.14. That this transition occurs at sexual maturity is described in more detail within the section “**A Real Species**”.

The transition from Equation 2.13a to Equation 2.13b is based only on the values of the two equations and not on arbitrary values. Here, then, is an excellent trigger to mark the onset of reproductive maturity and changes in the allocation of carbon to the canopy. Within simulations the onset of reproductive maturity is based on the first time Equation 2.13b is greater than or equal to Equation 2.13a, versus explicitly defining the age of reproductive maturity. The advantage of this method is that it is able to take into account environmental factors that affect when real-world plants reach reproductive maturity. With  $H_S$  dependant on the growth of a simulated tree, the greater a tree is shaded, the slower its growth, and thus the longer it takes for the tree to reach sexual maturity.

### *Allocation to Reproduction*

Within the world-wide compendium for forestry data compiled by Cannell (1982), there are several datasets that record the mass of propagules ( $M_P$ ). A basic model showing a relationship between propagule mass and growth ( $G_T$ ) was generated (Figure 2.8), represented by the formula

$$M_{P_T} = \phi_3 \beta_{13} G_{T_i}^{\alpha_{10}} \rightarrow M_{P_T} = \beta_{13} G_{T_i}^{\alpha_{10}} \quad (\text{Equation 2.21a and b})$$

where  $M_{P_T}$  is the total mass of all propagules produced by a given plant during a growth cycle,  $\beta_{13}$  and  $\alpha_{10}$  denote a species-specific normalization (allometric) constant and scaling exponent, respectively, and  $\phi_3$  is a species-specific value defining what fraction of total growth per year is dedicated to the construction of propagules. The maximum number of propagules ( $N_P$ ) that a plant can produce during any growth cycle is

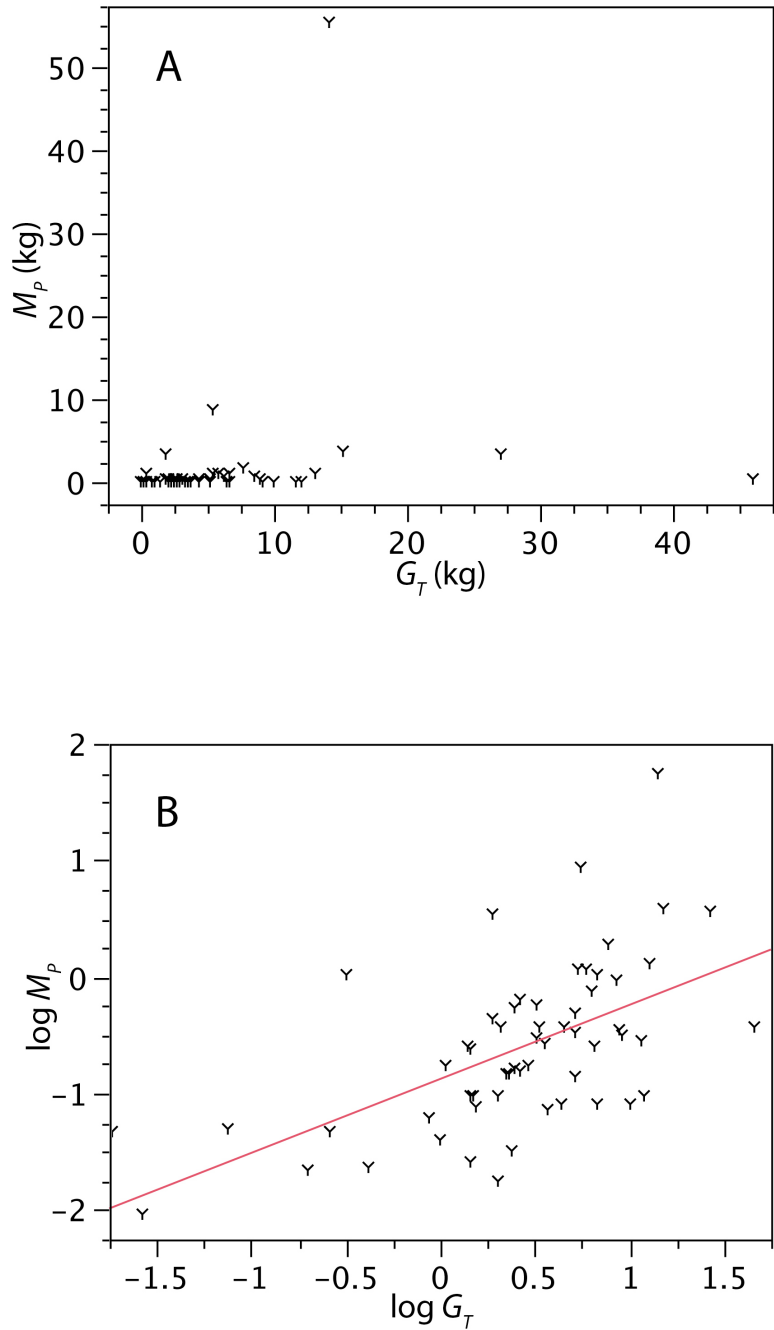


Figure 2.8: Average mass of all propagules above ground woody growth ( $M_p$ ) versus total above ground growth ( $G_T$ ) of all gymnosperms in the Cannell(1982) data set which have information regarding the mass of reproductive structures. A: simple plot of  $M_p$  versus  $G_T$ . B: log-log plot of  $M_p$  versus  $G_T$ , where the fit line is described by  $M_{P_T} = \phi_3 0.0997 G_{T_i}^{1.0978}$ , where  $\phi_3$  is equal to 1.0.

$M_{P_T}$  divided by the mass of an individual propagule ( $M_{P_{ideal}}$ ):

$$N_P = \frac{M_{P_T}}{M_{P_{ideal}}} \quad (\text{Equation 2.22})$$

The shift described by Equation 2.21 occurs when vegetative growth slows relative to an average value. Each species has a defined “growth memory” ( $m$ ) that determines how many years of previous growth a plant has experienced. For each iteration of a plant’s life, the average growth ( $G_{T_{average}}$ ), given by

$$G_{T_{average}} = \frac{\sum G_{T_{i-m}} \dots G_{T_i}}{m + 1} \quad (\text{Equation 2.23})$$

is compared against the current growth cycle’s growth ( $G_T$  in Equation 2.22). If  $G_{T_i} < G_{T_{average}}$ , the fractional difference ( $\phi_2$ ) between the two is determined:

$$\phi_4 = \frac{G_{T_i}}{G_{T_{average}}} \quad (\text{Equation 2.24})$$

Species can be seen as having levels of “selfishness” regarding the mass used to construct propagules. This selfishness factor ( $\phi_3$ ) represents the extent to which a plant invests more in reproduction than it requires for sustained vegetative growth. The conditions  $G_{T_i} < G_{T_{average}}$  and  $\phi_3 \geq \phi_4$  trigger a plant to set  $\phi_3 = 1.0$  and to divert as many resources to propagule production as possible, since the sudden reduction in growth could be due to severe changes in the environment or being rapidly overtapped by neighboring plants.

In summary, the selfishness factor quantifies the extent to which a plant invests more in reproduction than it requires for sustained vegetative growth. Specifically, if a plant is rapidly overtapped, annual growth rate will rapidly decrease, indicating that the plant risks death due to light deprivation. The level of  $\phi_3$  is the trigger point at which

the plant will shift from using Equation 2.21a to using Equation 2.21b. For example, if a species is 50% selfish (i.e.,  $\phi_3 = 0.5$ ), a plant would begin using Equation 2.21b instead of Equation 2.21a in an attempt to produce more propagules before it died due to light deprivation.

Using information on the mass of individual seeds one can estimate the total number of propagules produced, if one assumes all the  $M_P$  is used to produce seeds and not fruit flesh or cones. For example, the average mass of an individual seed of the Silver fir, *Abies alba*, is 0.000027kg (Goudwaard, 2006). Therefore,  $M_P$  is 1kg, 37,037 seeds can be produced, an unreasonable number for use in simulations.

To account for the mass of cones and other structures not directly measured by seed mass, the concept of  $M_P$  is any structure that is directly related to reproduction. For example, in the case of *A. alba*,  $M_P$  would include the mass of cones. Reproductive units were also combined so, instead of producing hundreds of cones, each filled with seeds, propagules represent a collection of cones and seeds, and from each propagule a single plant is produced. Upon germination, it is assumed that the new seedling should have the same mass as a single seed. Therefore, a certain mass of the propagule ( $M_{P_w}$ ) is lost. For example, if  $M_{P_{max}}$  is 0.6 kg and the average seed mass from the literature is 0.000027 kg,  $M_{P_w}$  would be equals 0.000045 kg.

### ***Propagule growth and dispersal —***

Propagule formation and growth on a canopy, like all aspects of Vida, are spatially explicit. Each propagule occupies a specific  $x, y, z$  location. Propagule location is defined by two variables ( $\phi_5, \phi_6$ ), each defining a fraction of the radius of the canopy. The value  $\phi_5$  represents the outermost fraction of the canopy radius propagules can occupy. The value  $\phi_6$  is the innermost fraction of the projected canopy radius at which propagules can be placed, e.g., the values  $\phi_5 = 1.0$  and  $\phi_6 = 1.0$  result in propagules

being placed at the canopy edge; the values  $\phi_6 = 1.0$ ,  $\phi_6 = 0.5$  result in propagules located at the outermost 50% of the projected canopy (Figure 2.9). The default setting allows propagules to develop anywhere on the canopy surface, i.e.,  $\phi_5 = 1.0$ ,  $\phi_6 = 0.0$ .

An ideal propagule mass is defined for each species. As propagules mature (whether over several iterations, or during a single iteration), their mass increases based on Equations 2.21 and 2.22, where each propagule will receive a certain amount of mass by dividing total propagule mass by propagule number. Using this method, it is possible for the mass of individual propagules to exceed  $M_{D_{ideal}}$ . Once  $M_D \geq M_{D_{ideal}}$ , the propagule is immediately dispersed.

There are five optional modes for propagule dispersal: (1) vertically from the canopy, (2) random dispersal, irrespective of the distance from a canopy, (3) random dispersal within a circle (with a specified radius) centered on the canopy, (4) random dispersion with a specified maximum distance orthogonal to the canopy-edge, and (5) the default setting, ballistic dispersion. Ballistic dispersal is done in such a way that it is assumed that it occurs in a vacuum, and that propagules pass through canopies and stems. Dispersal distance is governed by the launch angle relative to the horizontal ( $\theta$ ) and the initial velocity of the propagule ( $v$ ). In the default setting,  $\theta = 45^\circ$  and  $v = 5$  m/s. Noting that drag is neglected, the distance traveled is calculated using the formula

$$\text{Distance} = (v \cos \theta / g) \{ v \sin \theta + [v \sin \theta^2 + 2gz]^{1/2} \} \quad (\text{Equation 2.25})$$

where  $g$  is the acceleration due to gravity (9.81 m/s<sup>2</sup>) and  $z$  is the height of the propagule above ground.

The absolute maximum number of propagules a given tree can produce is limited by values provided at the start of a simulation. This limitation provides a cap to deal with computational limitations.

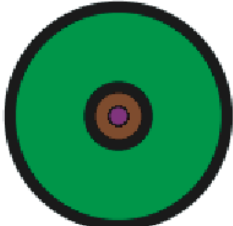
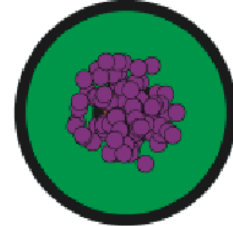
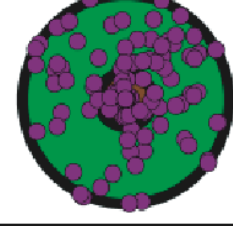
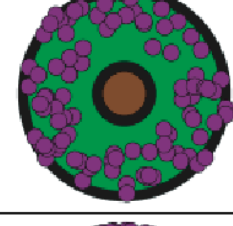
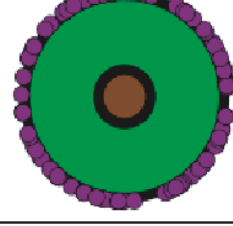
Description	Setting	Image
A	[0.0,0.0]	
B	[0.5,0.0]	
C	[1.0,0.0]	
D	[1.0,0.5]	
E	[1.0,1.0]	

Figure 2.9: Polar views of simulated trees showing examples of propagule (purple circles) formation on canopies (green circles). Stems (brown) are visible simply as a visual aid. A) Propagule formation is limited to the center. B) Propagule formation occurs on the inner 50% of the canopy. C) Propagule formation occurs over the entire surface of the canopy. D) Propagule formation occurs over the outer 50% of the canopy. E) Propagule formation occurs only along the outermost edge of the canopy.

## ***Mortality***

There are many ways in which an individual plant can die within a simulated world: (1) a propagule can fail to germinate, (2) if a propagule is dispersed outside of the boundaries of the world-space, (3) if a propagule lands on a location occupied by another plant or propagule, the smaller of the two objects (plant or propagule) dies, (4) if two stems grow and touch each other, the plant with the smaller mass dies, (5) if a plant exceeds its critical buckling height (calculated on the basis of the Euler-Greenhill formula (Greenhill, 1881; see Niklas and Spatz, 2006), (6) random death independent of propagule/plant size (to mimic stochastic processes such as tree fall or fire), (7) age-dependent death where the probability of death increases with age (to mimic increased risks of death by disease or some other age-dependent process), and (8) light deprivation resulting from overtopping canopies. Each of these methods of dying falls into one of three categories: basic physics, growth constraints, and stochastic processes.

## ***Death due to Physical Laws***

Within simulations, no two objects are allowed to occupy the same location. The exception to this is that canopies can become intermeshed. When there is a situation when two objects overlap, the object with the smaller mass dies. For example, a tiny seedling could be crushed by a massive coconut-like propagule. Likewise, a newly dispersed propagule's  $x$  and  $y$  location within the simulation might overlap with the trunk of a massive tree. In situations in which equally massed objects overlap, one is randomly chosen for death.

Because the simulated world space has defined edges, any object that extends off of the world-space dies. For example, propagules that are dispersed off of the simulation space are immediately killed, and any tree who's stem extends off the world-space is

also killed. The exception to this rule is that canopies can extend off the world-space, and continue to receive light.<sup>7</sup>

Trees can also die due to stem buckling, if their height exceeds the Euler-Greenhill critical buckling height (Greenhill, 1881; Niklas, 2006):

$$H_{S_{Critical}} = 0.79 \left( \frac{E}{g\rho_s} \right)^{\frac{1}{3}} \left( D_s^{\frac{2}{3}} \right) \quad (\text{Equation 2.26})$$

where  $E$  is the Young's modulus for the stem,  $g$  is the gravity,  $\rho_s$  is the density of the stem, and  $D_s$  is the diameter of the stem.

### ***Stochastic Mortality***

Without clear data on real-world mortality, test simulations were run to manually alter the rate of stochastic death in the simulation space until no more than one tree out of 100 lived to reach 600 years of age within the simulated world. The value arrived at means that every plant in a simulation has a 0.75% chance of dying during each iteration of a simulation.

### ***Growth Constraints: Lack of light***

Death due to insufficient light caused by overtopping plants shading an individual was covered in the section discussing how  $G_T$  was calculated. To recapitulate, each species is defined by a minimum fraction of the projected canopy area that must receive sunlight. Currently, all species must have 20% or more of their projected canopy area exposed to full light to survive. This calculation is complicated by the fact that each

---

<sup>7</sup> It should be noted that individuals growing on the edges are in interesting situations where they encounter less competition due to shading, but that a percentage of their propagules are wasted by being dispersed off world. Therefore, growing along an edge is beneficial to the individual plant, but that individual's chances of reproducing successfully are reduced.

species also allows a certain fraction of light to pass through its canopy (default for each species is 2%). For example, if a plant is completely overtapped by a larger plant, the smaller plant's canopy would receive only 2% of the available solar energy. If a plant is shaded by only one other plant, the amount of shading is directly calculated using hemispherical canopy geometry. If, however, a plant is shaded by two or more plants, a Monte-Carlo method is employed to estimate total shading.

### ***Growth Constraints: Senescence***

Like stochastic mortality, there is little empirical data to model senescence. Vida's senescence routines assume that an organism's vigor decreases over time due to damage caused by external factors (physical damage, viruses, bacteria, etc.) that eventually exceeds the organism's rate of growth and repair. One can think of this as a Red Queen (not to be confused with Red Queen Hypothesis proposed by van Valen, 1973) model of senescence; when an organism is young, it can outgrow the rate of damage, but as its growth slows—and the rate of damage remains constant—death is inevitable.

To model senescence, a given tree's fastest growth in height ( $G_{H_{\max}}$ ) is recorded. Its average increase in height ( $G_{H_{\mu}}$ ) over a moving 'growth memory' window is calculated every iteration a plant grows. These values are used to determine what the fraction of  $G_{H_{\max}}$  the current  $G_{H_{\mu}}$  is:

$$\theta_7 = \frac{G_{H_{\mu}}}{G_{H_{\max}}} \quad (\text{Equation 2.27})$$

If at any point  $\theta_7$  drops below a defined value ( $\theta_8$ ), the tree in question enters a second round of stochastic mortality. For example, if a given tree's growth has slowed to a point that  $\theta_7 < \theta_8$ , and if the stochastic mortality value is 0.75%, its overall chance of dying due to senescence and stochastic death doubles to 1.5%.

To determine reasonable values of  $\theta_8$ , test simulations were run using different

values. Simulations were initialized with 100 trees and various values of  $\theta_8$  were used until all trees survived to be at least  $H_{S_{\max}}$ , but died before exceeding  $H_{S_{\max}} + 5$ .

### *A Real Species: Abies alba*

Out of the six hundred and seventy-five entries in the Cannell database (Cannell, 1982), one entry proved particularly well documented. A single managed *Abies alba* population, with an initial population density of 25,000 plants/hectare, was observed and documented every five years, starting at the tenth year. The dataset concluded on the 95<sup>th</sup> year, providing 18 data points for most variables.

*Abies alba*, commonly called the silver fir, is native to Europe and primarily grows in mountainous regions stretching from Spain in the west, to Bulgaria and Greece in the east (Figure 2.10). In general, as one moves into lower latitudes, *A. alba* is found in higher elevations, forming belts 500 to 600 m wide within the areas with the densest growth (Wolf, 2003). *A. alba* is shade tolerant, and young trees are able to survive under tree canopies for decades (Niinemets 2006). When a gap appears in the canopy, these understory trees rapidly fill the space.

The silver fir is the tallest species of the genus. Trees can reach ages of 500 to 600 years old (Wolf 2003), reach heights of 45 to 55 m (Goudwaard, 2006) and have trunk diameters (DBH) of 150 to 200 cm (Wolf, 2003). Trees become reproductively mature between 25 and 35 years when isolated, whereas trees in a forest normally reach reproductive maturity between 60 and 70 (Wolf, 2003), with each seed weighing an average of 0.027 g (Goudwaard, 2006).

Using the Cannell dataset, standardized major axis (SMA, also known as reduced major axis) regression analyses of bivariate plots of plant height ( $H_S$ ), trunk diameter ( $D_S$ ), canopy, stem and total tree mass ( $M_L$ ,  $M_S$ , and  $M_T$ ), and annual canopy and stem growth rates ( $G_L$  and  $G_S$ ) were determined. The numerical values of these regressions

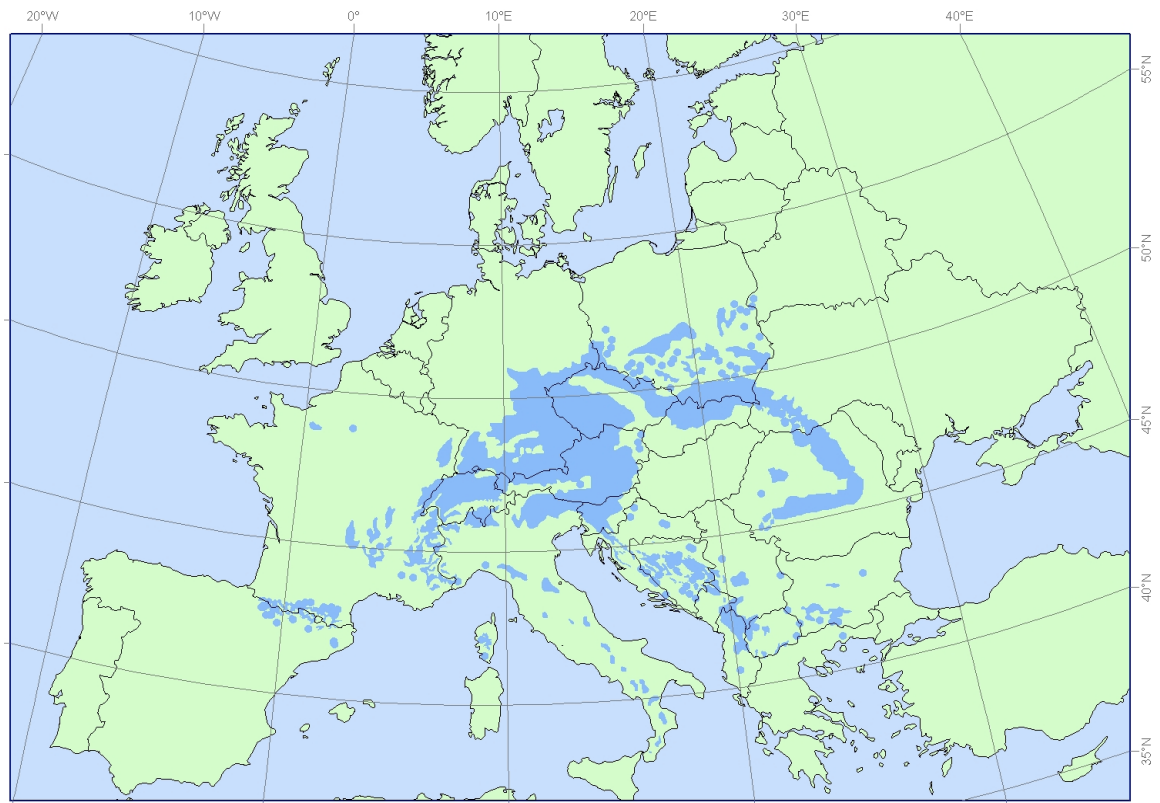


Figure 2.10: Distribution of *A. alba*, denoted in blue, in Europe as of 2004 (Wolf, 2004).

were used as input values in the generalized allometric formula  $\log Y_2 = \log \beta \pm \alpha \log Y_1$ , where  $Y_1$  and  $Y_2$  are interdependent variables (Figures 2.11-2.14) (Niklas, 1994; Warton, 2002, 2006).

As previously noted, close examination of the data indicated that the transition described by Equations 2.13 and 2.14 happens at the same time (within the time frames available in the dataset), i.e. after approximately 25 years of growth. As mentioned, Wolf (2003) reports that *A. alba* becomes reproductively mature after 25 to 35 years of growth in unshaded environments. Having both the onset of reproductive maturity and the transition happen at the same time as a result of some event is reasonable, given their empirical overlapping timeframes. For a simulation, one could simply define the age at which plants reach reproductive maturity and use that age as the trigger for the transition in carbon allocation to the canopy. However, doing so would not allow one to easily model subtleties regarding the onset of reproductive maturity. While *A. alba* grown in unshaded environments reaches reproductive maturity between 25 and 35 years of age, shaded trees growing in forests become reproductively mature as late as 60 to 70 years of age. Clearly, providing a fixed age at which plants become reproductively mature is not an ideal solution.

An examination of the relationship between stem height relative to diameter, as defined by Equation 2.13, offers a better solution. Table 2.1 shows values for  $H_S$  using both Equation 2.13a and Equation 2.13b in comparison to empirically reported values of  $H_S$  for *A. alba* from Cannell (1982). The point at which Equation 2.13b results in values for  $H_S$  that exceed those from Equation 2.13a represents a permanent change in how  $H_S$  is calculated in that equation 2.13a is replaced by 2.13b. The timing of this transition empirically corresponds with the transition in carbon allocation to the canopy as defined by Equation 2.14. For this reason, a basic model was constructed such that

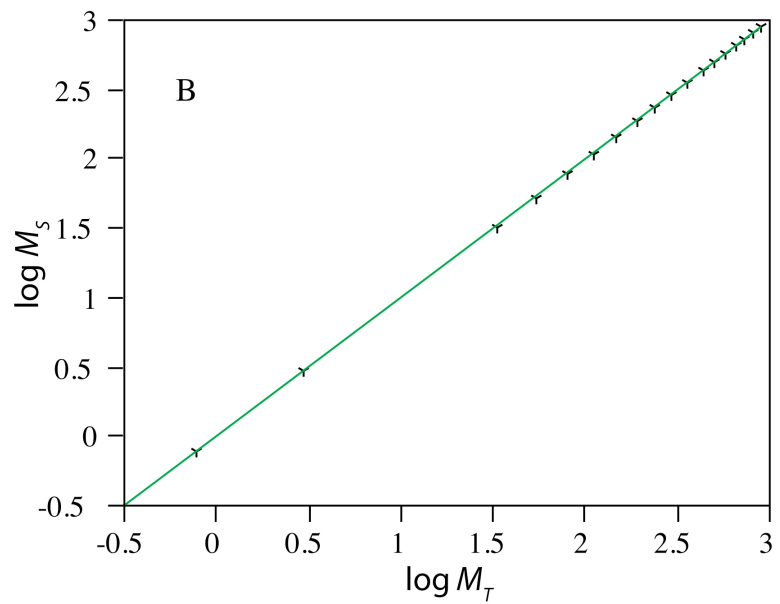
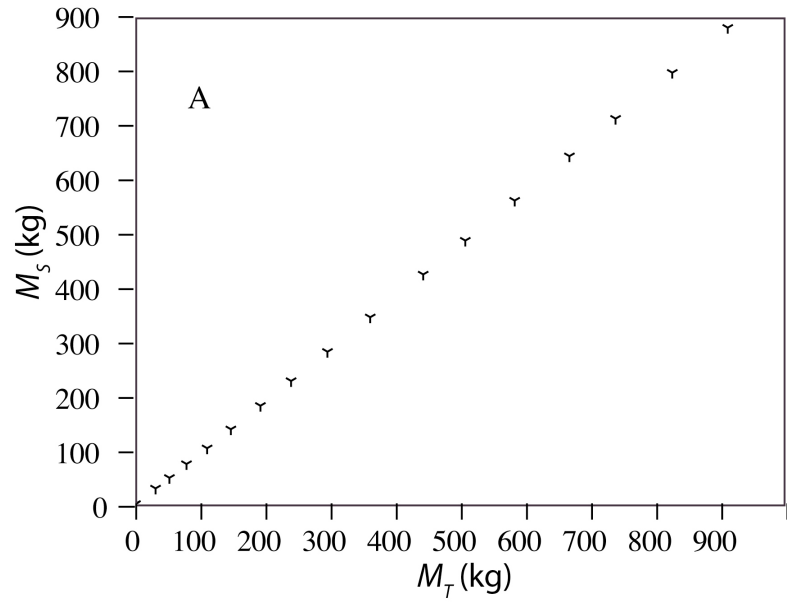


Figure 2.11: Average mass of all above ground woody growth ( $M_s$ ) verses the total above ground mass ( $M_T$ ) of a managed forest of *Abies alba*. A: simple plot of  $M_s$  versus  $M_T$ . B: log-log plot of  $M_s$  versus  $M_T$ , where the fit line is described by

$$M_s = 0.941 M_T^{1.0013}$$

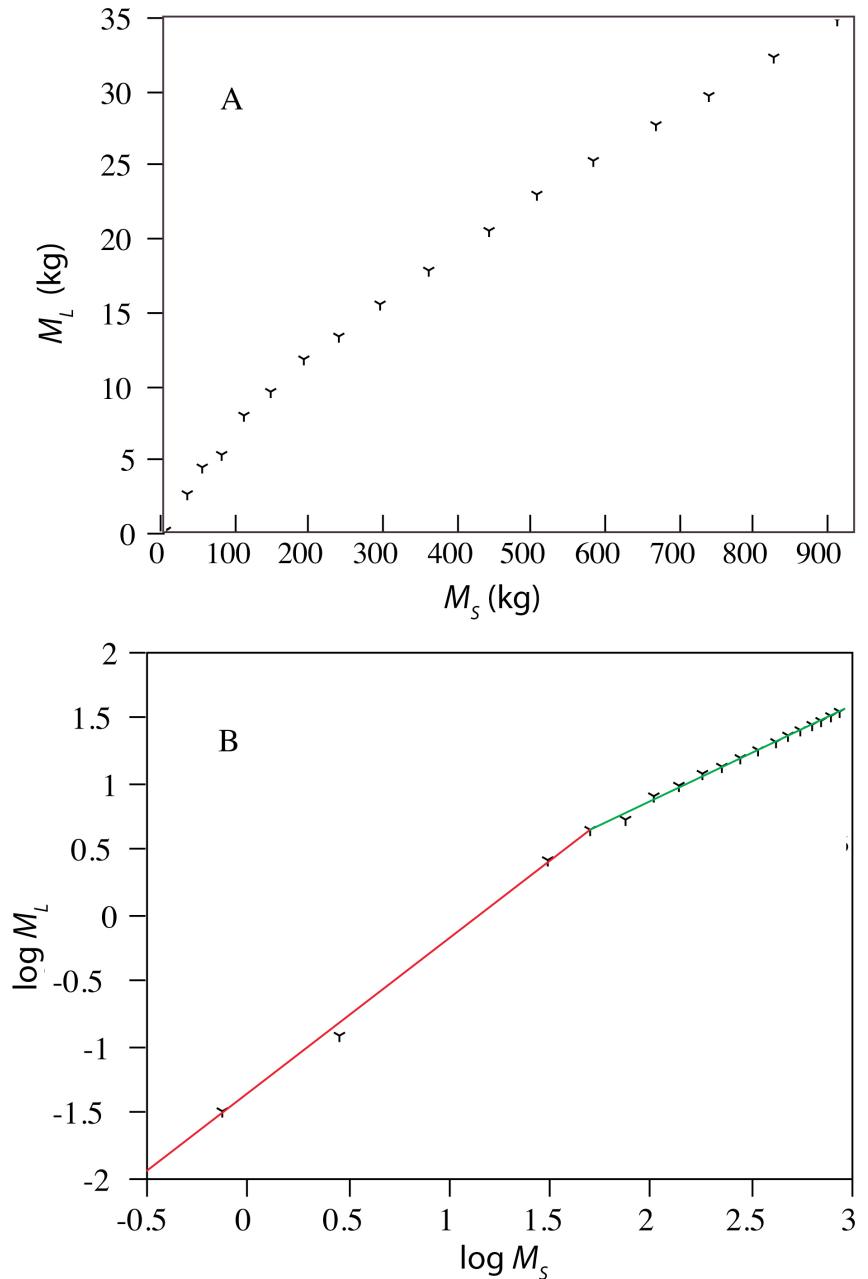


Figure 2.12: Average mass of the canopy ( $M_L$ ) versus the all above ground woody growth ( $M_S$ ) of a managed forest of *Abies alba*. A: simple plot of  $M_L$  versus  $M_S$ . B: log-log plot of  $M_L$  versus  $M_S$ , showing two distinct, where the fit lines are described by

$$M_{L_{young}} = 0.0397 M_S^{1.1982} \text{ and } M_{L_{mature}} = 0.2483 M_S^{0.7306}$$

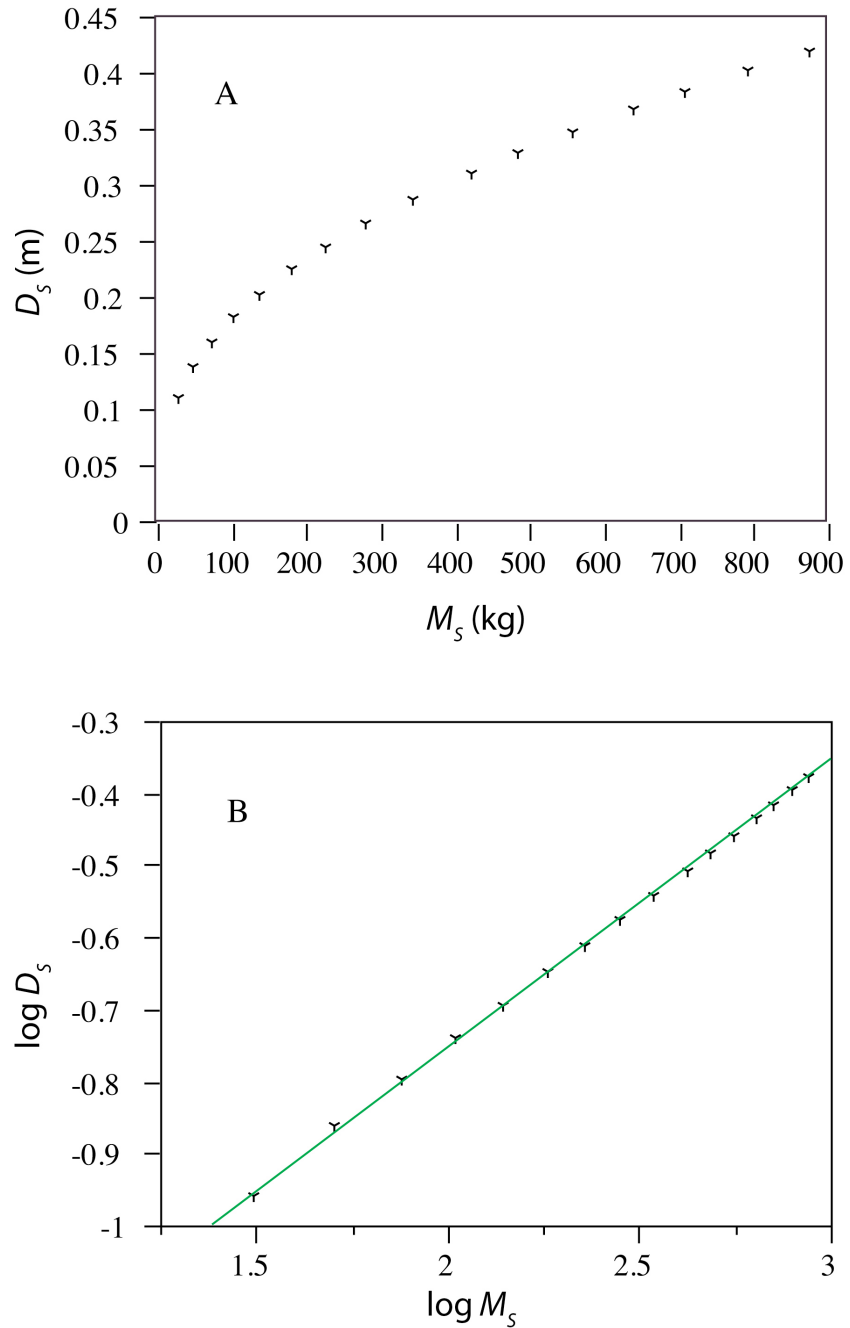


Figure 2.13: Average Diameter at Breast Height ( $D_s$ ) versus mass of all above ground woody growth ( $M_s$ ) of a managed forest of *Abies alba*. A: simple plot of  $D_s$  versus  $M_s$ . B: log-log plot of  $D_s$  versus  $M_s$ , where the fit line is described by  $D_s = 0.029 M_s^{0.3942}$

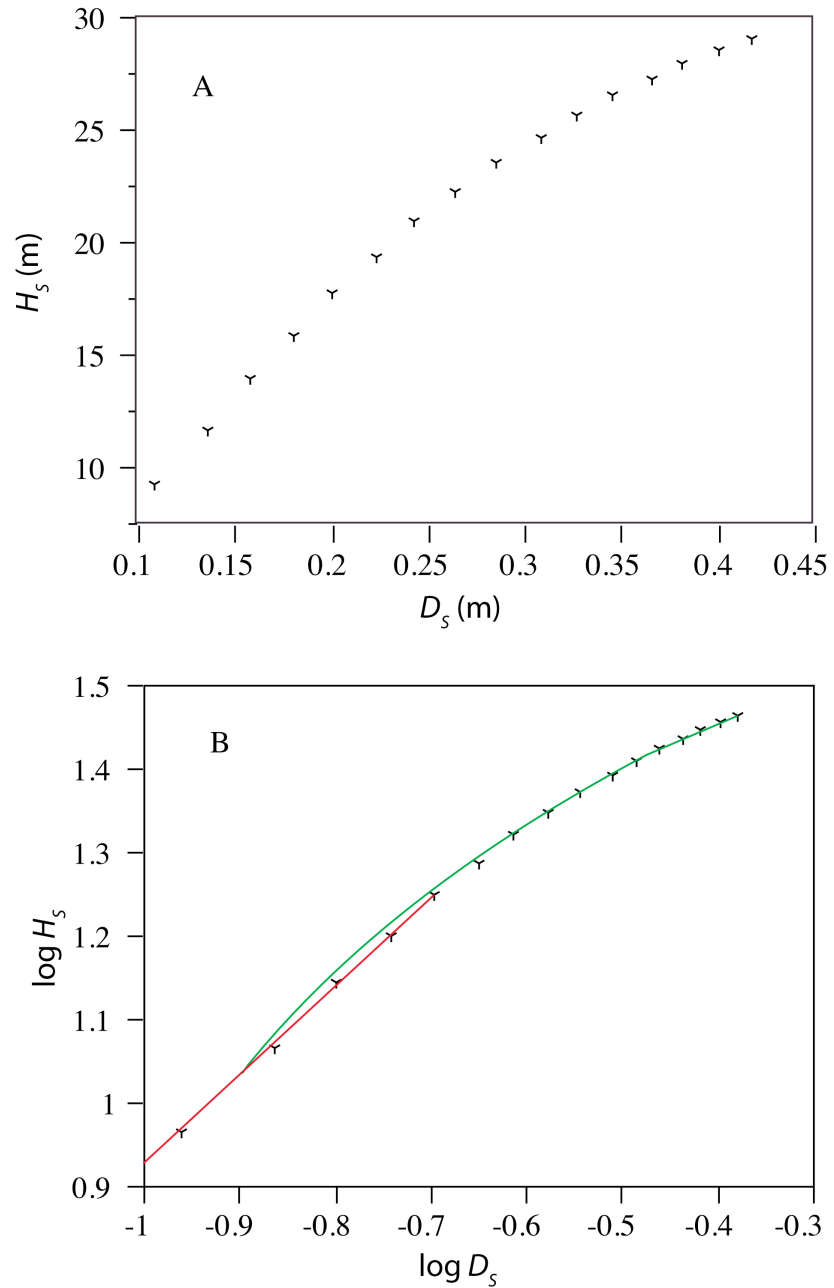


Figure 2.14: Average height of a tree ( $H_s$ ) versus the Diameter at Breast Height (DBH) ( $D_s$ ) of a managed forest of *Abies alba*. A: simple plot of  $H_s$  versus  $D_s$ . B: log-log plot of  $H_s$  versus  $D_s$ , showing two distinct, where the fit lines are described by

$$H_{S_{young}} = 100.0642D_s^{1.0809} \text{ and } H_{S_{mature}} = 42.6982 + 15.5080\ln D_s$$

Table 2.1 Values of  $H_S$  generated through the use of  $H_S = \beta_7 D_S^{\alpha_7} - \beta_8 \rightarrow H_S = \beta_9 + \beta_{10} \ln D_S$  (Equation 2.13), where the left hand side of the equation (Equation 2.13a) is  $H_S$  for *A. alba* younger than the age of sexual maturity, and the right side of the equation (Equation 2.13b) is  $H_S$  for *A. alba* at the age of maturity, or older. Values corresponding with the onset of sexual maturity are in bold. Units for variables:  $H_S$  (m).

Cycle	Actual $H_S$	Predicted $H_{S\ young}$	Predicted $H_{S\ mature}$
10	ND	1.92244	-14.005
15	ND	3.40142	-5.8187
20	9.2	9.54321	8.98244
<b>25</b>	<b>11.6</b>	<b>11.7526</b>	<b>11.9702</b>
30	13.9	13.8716	14.3485
35	15.8	15.9587	16.3594
40	17.7	17.9816	18.0717
45	19.3	20.1346	19.6942
50	20.9	22.0832	21.0196
55	22.2	24.1292	22.2908
60	23.5	26.27	23.5104
65	24.6	28.6324	24.7459
<b>70</b>	<b>25.6</b>	<b>30.339</b>	<b>25.5765</b>
75	26.5	32.1886	26.4256
80	27.2	34.0848	27.2468
85	27.9	35.5802	27.8628
90	28.5	37.3091	28.5436
95	29	38.9018	29.1433

Table 2.2: Values generated by a simple Microsoft Excel spreadsheet parameterized using empirical allometric relationships derived from data reported in Cannell, 1982. Values in red indicate when a transition in formula occurs. Units for variables:  $M_T$  (kg),  $M_S$  (kg),  $M_L$  (kg),  $D_S$  (m) and  $H_S$  (m).

Cycle	Actual MT	Predicted		Predicted		Predicted		Predicted		Predicted	
		M <sub>L</sub>	Actual M <sub>S</sub>	M <sub>L</sub>	Actual M <sub>S</sub>	M <sub>L</sub>	Actual DS	D <sub>S</sub>	Actual H <sub>S</sub>	H <sub>S,mean</sub>	H <sub>S,actual</sub>
10	0.792	<b>0.773</b>	0.760	<b>0.745</b>	0.032	<b>0.028</b>	0.202	ND	0.026	ND	-14.005
15	3.017	<b>2.983</b>	2.897	<b>2.844</b>	0.120	<b>0.138</b>	0.535	ND	<b>0.044</b>	ND	-5.819
20	33.870	<b>34.556</b>	31.279	<b>32.028</b>	2.590	<b>2.499</b>	3.119	0.110	<b>0.114</b>	9.200	9.543
25	55.183	<b>56.758</b>	50.780	<b>52.217</b>	4.404	<b>4.480</b>	<b>4.453</b>	0.137	<b>0.138</b>	11.600	<b>11.753</b>
30	81.388	<b>82.990</b>	76.130	<b>77.052</b>	5.258	<b>7.131</b>	<b>5.912</b>	0.159	<b>0.161</b>	13.900	13.872
35	113.043	<b>114.619</b>	105.122	<b>107.069</b>	7.921	<b>10.565</b>	<b>7.513</b>	0.182	<b>0.183</b>	15.800	15.959
40	149.533	<b>150.948</b>	140.000	<b>141.683</b>	9.533	<b>14.764</b>	<b>9.214</b>	0.202	<b>0.204</b>	17.700	17.982
45	194.924	<b>196.004</b>	183.182	<b>184.756</b>	11.742	<b>20.274</b>	<b>11.179</b>	0.225	<b>0.227</b>	19.300	20.135
50	242.052	<b>242.671</b>	228.764	<b>229.491</b>	13.288	<b>26.268</b>	<b>13.091</b>	0.244	<b>0.247</b>	20.900	22.083
55	297.925	<b>297.885</b>	282.453	<b>282.543</b>	15.472	<b>33.677</b>	<b>15.232</b>	0.265	<b>0.268</b>	22.200	24.129
60	363.617	<b>362.685</b>	345.851	<b>344.935</b>	17.766	<b>42.742</b>	<b>17.615</b>	0.287	<b>0.290</b>	23.500	26.270
65	444.945	<b>442.773</b>	424.482	<b>422.198</b>	20.463	<b>54.415</b>	<b>20.409</b>	0.310	<b>0.314</b>	24.600	28.632
70	509.618	<b>506.375</b>	486.693	<b>483.652</b>	22.925	<b>64.007</b>	<b>22.532</b>	0.328	<b>0.332</b>	25.600	30.339
75	585.447	<b>580.870</b>	560.231	<b>555.720</b>	25.216	<b>75.560</b>	<b>24.931</b>	0.347	<b>0.350</b>	26.500	32.189
80	669.510	<b>663.373</b>	641.864	<b>635.629</b>	27.646	<b>88.715</b>	<b>27.494</b>	0.367	<b>0.369</b>	27.200	34.085
85	740.404	<b>732.894</b>	710.774	<b>703.030</b>	29.630	<b>100.066</b>	<b>29.588</b>	0.383	<b>0.384</b>	27.900	35.580
90	827.505	<b>818.245</b>	795.264	<b>785.850</b>	32.240	<b>114.306</b>	<b>32.088</b>	0.402	<b>0.401</b>	28.500	<b>37.309</b>
95	912.695	<b>901.669</b>	877.930	<b>866.866</b>	34.766	<b>128.522</b>	<b>34.466</b>	0.419	<b>0.417</b>	29.000	<b>38.902</b>

the transition from using Equation 2.13a to 2.13b also served as a trigger to transition from Equation 2.14a to 2.14b.

Using these formulae and variables, it was possible to model the growth of a single *A. alba* tree using a Microsoft Excel spreadsheet (Table 2.2). Initial tests of the basic formulae (Equations 2.9, 2.11, 2.13, 2.14, 2.19 and 2.21 using the constants and exponents from Figures 2.7, 2.8, 2.11-2.14, and making transitions in Equations 2.13 and 2.14 as described above) showed an excellent correspondence with empirical data for the *A. alba* population reported in Cannell (1982). The initial tests only looked at time periods for which Cannell reported data, but did not allow for reiterative growth from year to year. Later tests included basic photosynthetic calculations for single plants. The final, fully functional version of Vida, which is able to simulate the growth of a single tree, groups of trees, and growth of mixed species, is discussed within chapters 3 and 4.

## REFERENCES

- CANNELL, M. G. R. 1982. *World Forest Biomass and Primary Production Data*. Academic Press, London, UK.
- CANTIANA, M. 1974. Experimental research into dendrometry and auxometry. Part II. Initial enquires concerning the biomass of the white fir. [in Italian] *Bulletin 5. Instit. Assestamento Forestale*. Univ. of Firenze, Italy.
- Centers for Disease Control and Prevention, National Center for Health Statistics. 30 May, 2000. CDC growth charts: United States. <http://www.cdc.gov/growthcharts/>.
- DEUSSEN, O., P. HANRAHAN, B. LINTERMANN, R. MECH, M. PHARR, AND P. PRUSINKIEWICZ. 1998. Realistic Modeling and Rendering of Plant Ecosystems. *Proceedings of the 25<sup>th</sup> annual conference on Computer graphics and interactive techniques*. 275-286.
- ENQUIST, B. J. AND K. J. NIKLAS. 2001a. Invariant Scaling Relations Across Tree-Dominated Communities. *Nature*. 410: 655-660.
- ENQUIST, B. J. AND K. J. NIKLAS. 2001b. Supplementary Information for “Invariant Scaling Relations Across Tree-Dominated Communities.” *Nature*. 410: 655-660.
- GOUDWAARD, L. 2006. Tree factsheet: *Abies alba*. Wageningen University Forest Ecology and Forest Management Group.
- GREENHILL, A. G. 1881. Determination of the greatest height consistent with stability that a vertical pole or mast can be made, and of the greatest height to which a tree or green proportions can grow. *Proceedings of the Cambridge Philosophical Society*. 4: 65-73.

- HASEGAWA, Y., Y. YAMADA, M. TAMURA, AND Y. NOMURA. 1991. Monte Carlo simulation of light transmission through living tissues. *Applied Optics*. 30(31):4515-4520.
- HAWKES, C. 2000. Woody Plant Mortality Algorithms: Description, Problems and Progress. *Ecological Modelling*. 126: 225-248.
- HUXLEY, J. S. 1932. *Problems of relative growth*. The Dial Press, New York.
- JENKINS, J. C, D. C. CHOJNACKY, L. S. HEATH, AND R. A. BIRDSEV. *Comprehensive Database of Diameter-based Biomass Regressions for North American Tree Species*. USDA Forest Service.
- LINTERMANN, B. AND O. DEUSSEN. 1998. A Modelling Method and User Interface for Creating Plants. *Computer Graphics Forum*. 17(1): 73-82.
- MANDELBROT, B. B. 1982. *The Fractal Geometry of Nature*. W.H. Freeman and Company.
- MARTELLI, A., A. M. RAVENSCROFT, AND D. ASCHER. 2005. *Python Cookbook, Second Edition*. O'Reilly Media, Inc.
- NAVAR, J. 2009. Allometric equations for tree species and carbon stocks for forests of northwestern Mexico. *Forest Ecology and Management*. 257: 427-434.
- NEUBURG, M. 1999. *RealBasic: The Definitive Guide*. O' Reilly and Associates, Inc.
- NIINEMETS, Ü. AND F. VALADARES. 2006. Tolerance to shade, drought, and waterlogging of temperate Northern Hemisphere trees and shrubs. *Ecological Monographs*. 76: 521-547.
- NIKLAS, K. J. 1994. *Plant Allometry: The Scaling of Form and Process*. University of Chicago Press, Chicago.
- NIKLAS, K. J. 2004. Plant allometry: is there a grand unifying theory? *Biological Reviews*. 79: 871-889.

- PRAHL, S. A., M. KEIJZER, S. L. JACQUES, AND A. J. WELCH. 1989. A Monte Carlo Model of Light Propagation in Tissue. *SPIE Institue Series IS 5*: 102-111.
- PRINGLE, J., AND A. LANCASTER. 2001. Unpublished code for PLANT.
- RICHTER, J. P. (ed) 1939. The Literary Works of Leonardo da Vinci, Volume 1. Oxford University Press.
- SHINOZAKI, K., K. YODA, K. HOZUMI, AND T. KIRA. 1964a. A Quantitative Analysis of Plant Form: The Pipe Model Theory. I. Basic Analysis. *Japanese Journal of Ecology*. 14(3): 97-105.
- SHINOZAKI, K., K. YODA, K. HOZUMI, AND T. KIRA 1964b. A Quantitative Analysis of Plant Form: The Pipe Model Theory. II. Further Evidence of the Theory and its Application in Forest Ecology. *Japanese Journal of Ecology*. 14(3): 133-139.
- TANENBAUM, A. S. 1992. *Modern Operating Systems*. Prentice-Hall, Inc.
- VAN VALEN, L. 1973. A New Evolutionary Law. *Evolutionary. Theory*. 1: 1-30.
- WALL, L., T. CHRISTIANSEN, AND J. ORWANT. 2000. *Programming Perl: Third Editon*. O'Reilly and Associates, Inc.
- WARTON, D. I., AND N. C. WEBER. 2002. Common slope tests for bivariate errors-in-variables. *Biometry Journal*. 44: 161 – 174.
- WARTON, D. I., I. J. WRIGHT, D. S. FALSTER, AND M. WESTOBY. 2006. Bivariate line-fitting methods for allometry. *Biological Reviews*. 81: 259 – 291.
- WILSON, B. C. AND G. ADAM. 1983. A Monte Carlo model for the absorption and flux distributions of light in tissue. *Medical Physics*. 10(6):824-830.
- WOLF, H. 2003. EUFORGEN Technical Guidelines for Genetic Conservation and Use for Silver Fir (*Abies alba*). International Plant Genetic Resource Institute, Rome, Italy.
- ZIANIZ, D., P. MUUKKONEN, R. MÄKIPÄÄ, AND M. MENCUCCINI. 2005. Biomass and Stem Volume Equations for Tree Species in Europe. *Silva Fennica Monographs 4*